

## **Supplementary Information**

# **Coherent control of thermal phonon transport in van der Waals superlattices**

Ruiqiang Guo<sup>1</sup>, Young-Dahl Jho<sup>2</sup> and Austin J. Minnich<sup>1,\*</sup>

<sup>1</sup> Division of Engineering and Applied Science, California Institute of Technology, Pasadena,  
California 91125, USA

<sup>2</sup> School of Electrical Engineering and Computer Science, Gwangju Institute of Science and  
Technology, Gwangju 61005, South Korea

---

\* Corresponding author, [aminnich@caltech.edu](mailto:aminnich@caltech.edu).

## Supplementary Notes

### Supplementary Note 1. Effect of strains on the $\kappa_L$ of the MoSe<sub>2</sub>/WS<sub>2</sub> superlattice

For the MoSe<sub>2</sub>/WS<sub>2</sub> superlattice, confining the two materials to one unit cell leads to 2% tensile and compressive in-plane strains in the WS<sub>2</sub> and MoSe<sub>2</sub> layers compared to their bulk counterparts, respectively. To evaluate the influence of the strains on thermal transport, we first optimize the lattice parameters of bulk WS<sub>2</sub> and MoSe<sub>2</sub> by applying the corresponding strains and allowing the cross-plane lattice constants to relax. The obtained cross-plane lattice constants of WS<sub>2</sub> and MoSe<sub>2</sub> are decreased and increased by 1%, respectively. As a result, the cross-plane lattice constant of the MoSe<sub>2</sub>/WS<sub>2</sub> superlattice is only 0.2% smaller than the average value of corresponding bulk crystals, a minor change compared to the in-plane ones.

We then calculate the  $\kappa_L$  of the two strained crystals, as shown in Figure S1. Compared to unstrained crystals, the in-plane thermal conductivity  $\kappa_{in}$  of the strained WS<sub>2</sub> at 300 K decreases from 153.5 to 129.3 W m<sup>-1</sup>K<sup>-1</sup> while the cross-plane one  $\kappa_{cross}$  increases from 3.9 to 4.2 W m<sup>-1</sup>K<sup>-1</sup>. For the MoSe<sub>2</sub>, the 2% compressive strain increases the  $\kappa_{in}$  and  $\kappa_{cross}$  at 300 K from 40.9 and 2.6 to 48.5 and 3.2 W m<sup>-1</sup>K<sup>-1</sup>, respectively. We now use the average value of  $\kappa_L$  in both bulk crystals to estimate that the  $\kappa_{in}$  of the MoSe<sub>2</sub>/WS<sub>2</sub> superlattice decreases by 9% due to the 2% in-plane strains. For the  $\kappa_{cross}$  of the superlattice, its variation is negligible considering the very small cross-plane strain. Therefore, the thermal anisotropy ratio  $\kappa_{in}/\kappa_{cross}$  of the strained superlattice may decrease by  $\sim 9\%$ . These minor deviations caused by the strain effect thus will not affect our discussion and conclusion.

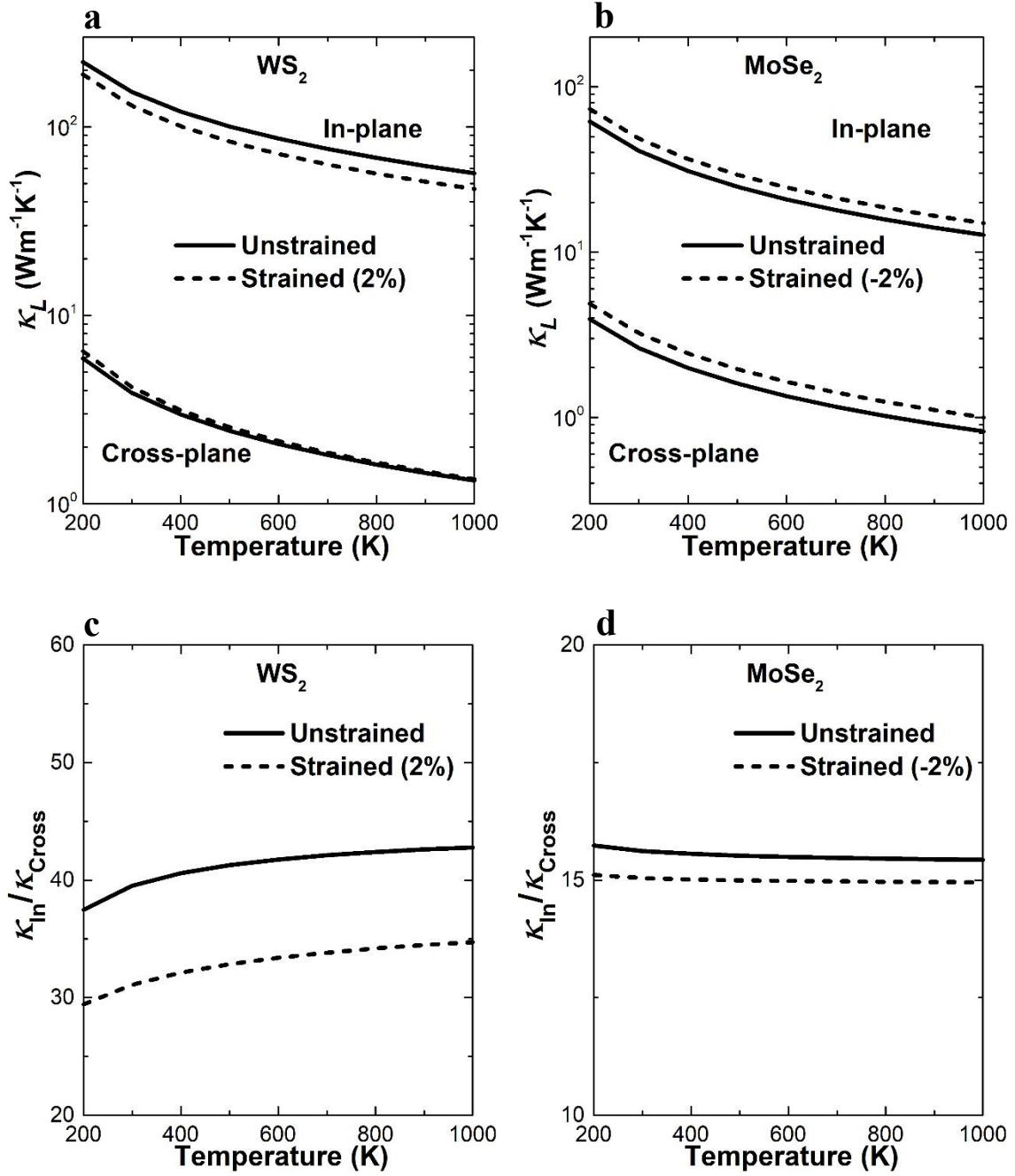


**Figure S1.** Effect of strains on thermal properties of bulk  $WS_2$  and  $MoSe_2$ . (a, b) In-plane (top) and cross-plane (bottom) thermal conductivity  $\kappa_L$  and (c, d) thermal anisotropy  $\kappa_{In}/\kappa_{Cross}$  versus temperature for bulk  $WS_2$  and  $MoSe_2$ , respectively.

## Supplementary Note 2. Effect of the impurity scattering on the $\kappa_L$ in TMDCs

The calculated  $\kappa_L$  are generally relatively higher or close to the corresponding maximum experimental data. In principle, the well-established *ab initio* BTE approach predicts the upper limit of  $\kappa_L$ , representing that of perfect crystals. Prior *ab initio* calculations have reproduced experimental measurements for many materials<sup>1-7</sup>, many of which were isotropic and for which high-quality samples were available. Experimental results may vary substantially due to sample impurities, geometries and measurement techniques. For anisotropic materials, the determination of the in- and cross-plane thermal conductivity on the same sample can be challenging.

Impurities may have a significant impact on the measured thermal conductivity values. Although the purity of currently synthesized samples can be larger than 99%, impurity scattering may still significantly suppress phonon transport, particularly for materials with high thermal conductivities. As a typical example, 0.1% boron impurities in WS<sub>2</sub> can decrease the  $\kappa_{in}$  and  $\kappa_{cross}$  to 114.6 and 3.3 W m<sup>-1</sup>K<sup>-1</sup> at 300 K, a reduction of 25.3% and 15.4% respectively. The impurity scattering more strongly suppresses the  $\kappa_{in}$  due to the significant contribution of higher frequency modes along this crystal plane, possibly explaining why our results agree better with the  $\kappa_{cross}$  reported by Jiang et al<sup>8</sup>. The  $\kappa_{in}$  and  $\kappa_{cross}$  are mainly contributed by phonons spanning a broader (0-7 THz) and narrower (0-2 THz) frequency range, respectively.

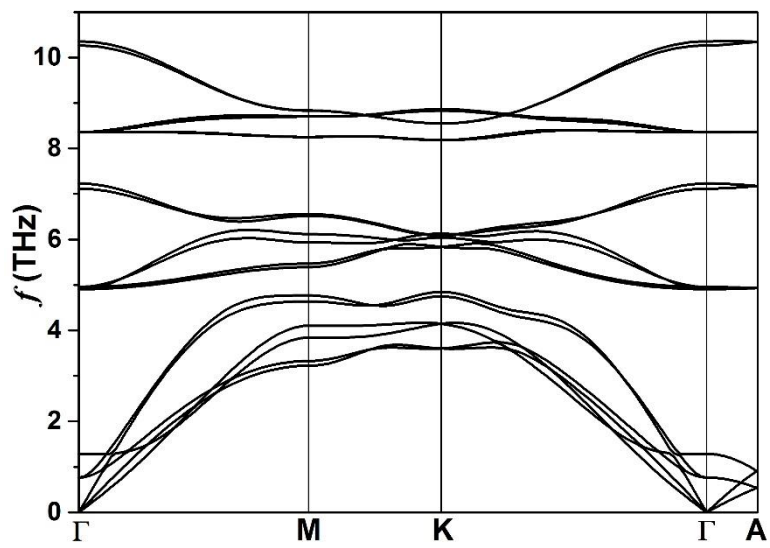


**Figure S2.** Phonon dispersion of bulk MoSe<sub>2</sub>.

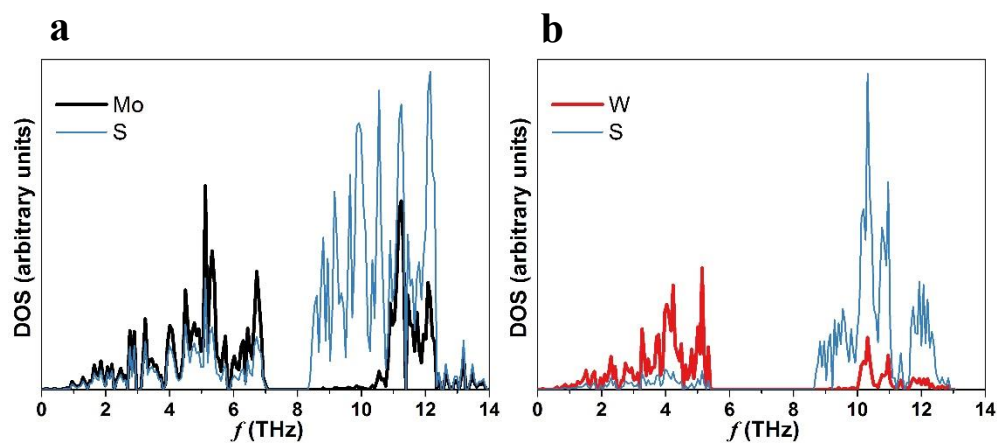


**Figure S3.** Partial phonon density of states of the bulk (a) MoS<sub>2</sub> and (b) WS<sub>2</sub>. Heavier atoms (Mo, W) dominate the lattice vibrations at low frequencies while lighter ones (S) dominate those at high frequencies.

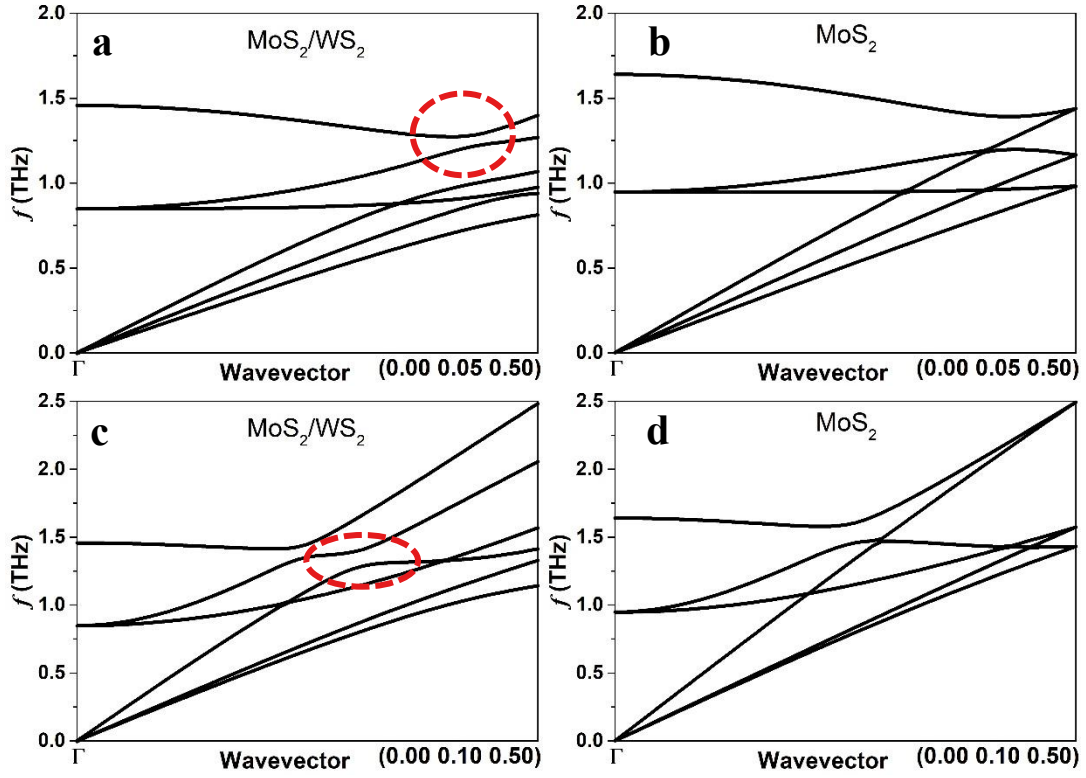


**Figure S4.** Anticrossing effects in superlattices. Phonon dispersions of the (a, c)  $\text{MoS}_2/\text{WS}_2$  and (b, d)  $\text{MoS}_2$  along two different Brillouin paths. The clear anticrossing effects (marked by red dashed lines) for the  $\text{MoS}_2/\text{WS}_2$  superlattice substantially reduce group velocities.

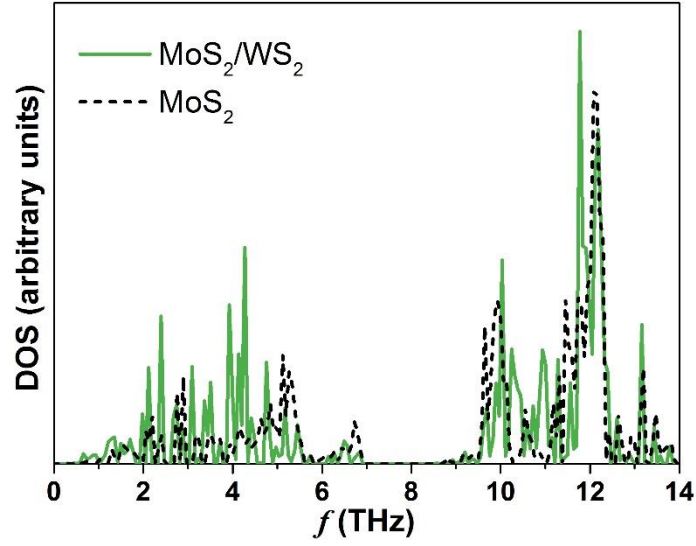


**Figure S5.** Phonon density of states projected along the  $z$  axis for the  $\text{MoS}_2/\text{WS}_2$  superlattice and bulk  $\text{MoS}_2$ . Several sharp peaks for  $f < 6$  THz in the density of states of the  $\text{MoS}_2/\text{WS}_2$  superlattice result from the occurrence of band gaps at zone edges and anticrossings inside the zone.

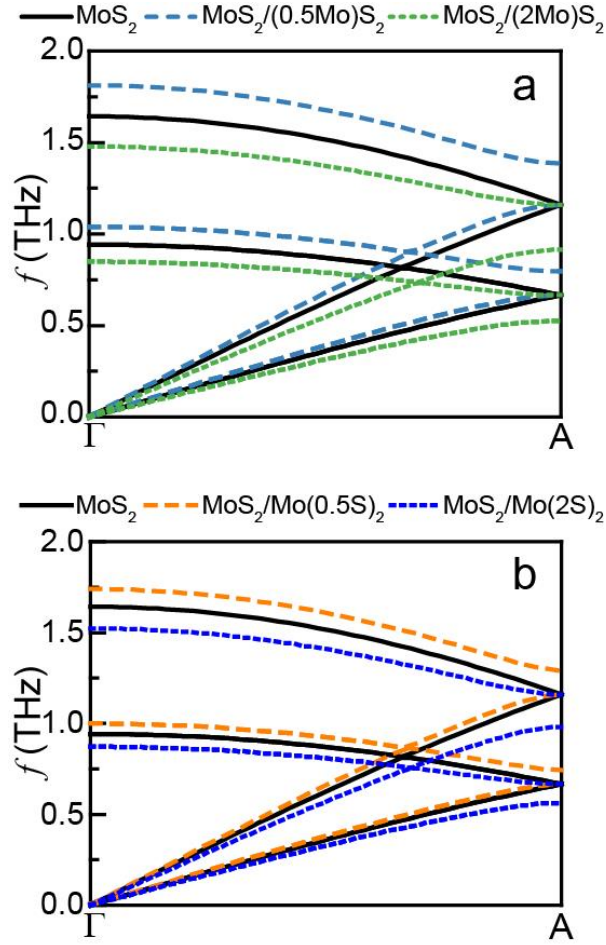


**Figure S6.** Effects of mass ratio on phonon dispersions. Phonon dispersions along the  $\Gamma$ A direction for (a)  $\text{MoS}_2$ ,  $\text{MoS}_2/(0.5\text{Mo})\text{S}_2$  (half the atomic mass of Mo is used) and  $\text{MoS}_2/(2\text{Mo})\text{S}_2$  (twice the atomic mass of Mo), and (b)  $\text{MoS}_2$ ,  $\text{MoS}_2/\text{Mo}(0.5\text{S})_2$  (half the atomic mass of S) and  $\text{MoS}_2/\text{Mo}(2\text{S})_2$  (twice the atomic mass of S). Increasing the mass difference leads to larger band gaps.

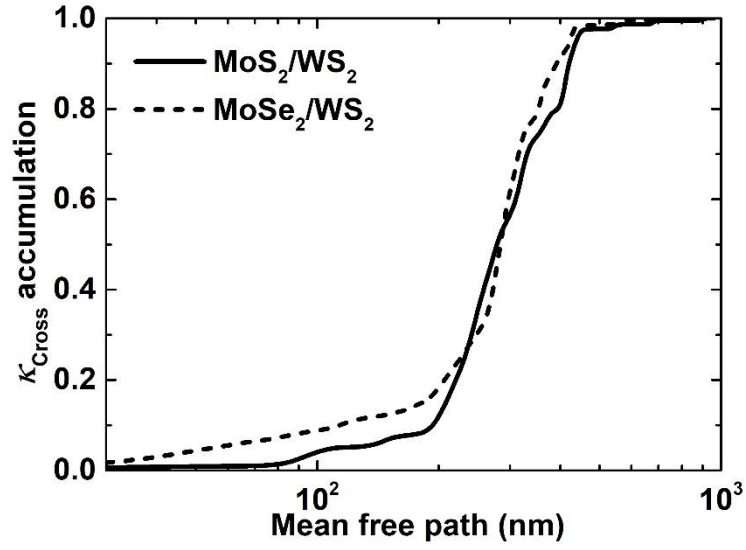


**Figure S7.**  $\kappa_{\text{Cross}}$  accumulation as a function of phonon mean free path for the MoS<sub>2</sub>/WS<sub>2</sub> and MoSe<sub>2</sub>/WS<sub>2</sub> superlattices. Most heat is carried by phonons with coherence lengths far exceeding the periodicity of around 1.2 nm for the superlattices.

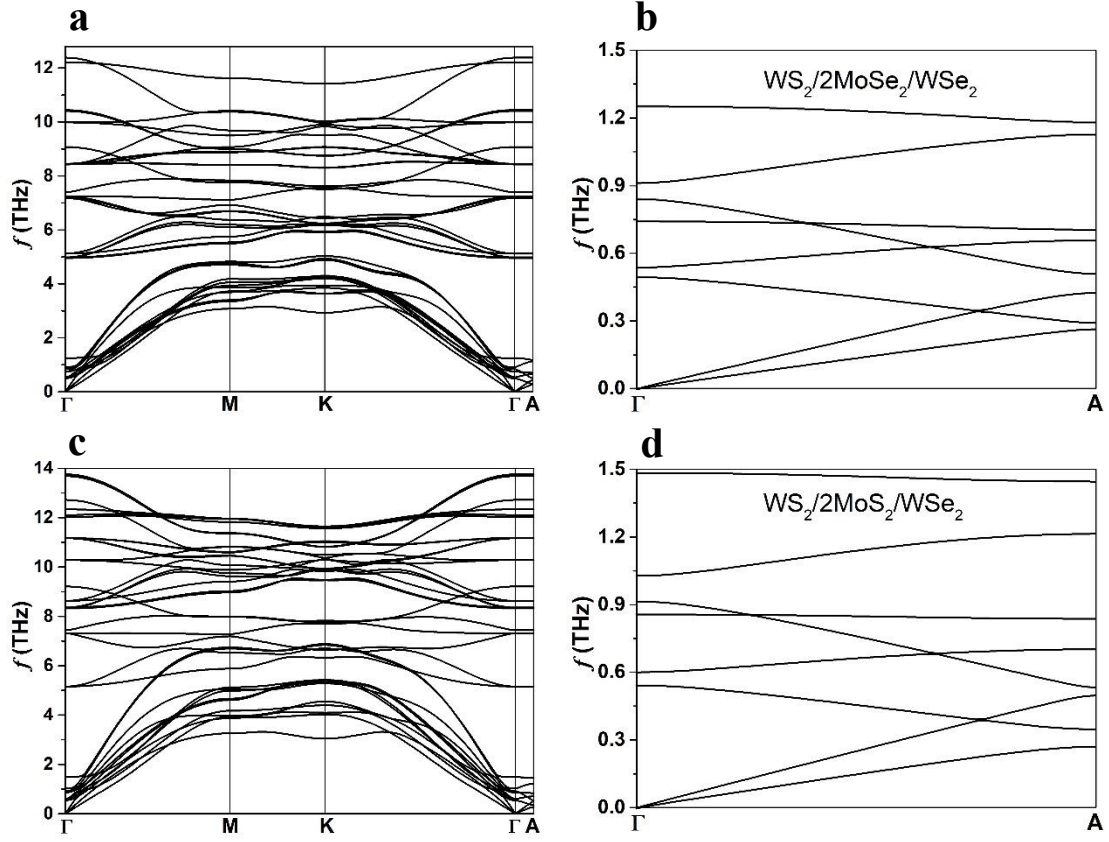


**Figure S8.** Phonon dispersions of the (a, b)  $\text{WS}_2/2\text{MoSe}_2/\text{WSe}_2$  and (c, d)  $\text{WS}_2/2\text{MoS}_2/\text{WSe}_2$  heterostructures. Zoom-ins of the twelve low-lying phonon branches along the  $\Gamma\text{A}$  direction are shown in (b) and (d). More significant band splitting along the in-plane directions and larger band gaps at zone edges are observed for the phonon dispersion of the  $\text{WS}_2/2\text{MoS}_2/\text{WSe}_2$  heterostructure.

## Supplementary References

1. Ward, A., Broido, D., Stewart, D. A. & Deinzer, G. Ab initio theory of the lattice thermal conductivity in diamond. *Phys. Rev. B* **80**, 125203 (2009).
2. Esfarjani, K., Chen, G. & Stokes, H. T. Heat transport in silicon from first-principles calculations. *Phys. Rev. B*, 085204 (2011).
3. Tian, Z. *et al.* Phonon conduction in PbSe, PbTe, and PbTe<sub>1-x</sub>Se<sub>x</sub> from first-principles calculations. *Phys. Rev. B* **85**, 184303 (2012).
4. Lindsay, L., Broido, D. & Reinecke, T. Thermal conductivity and large isotope effect in GaN from first principles. *Phys. Rev. Lett.* **109**, 095901 (2012).
5. Wang, X. & Huang, B. Computational Study of In-Plane Phonon Transport in Si Thin Films. *Sci. Rep.* **4**, 6399 (2014).
6. Li, W. & Mingo, N. Lattice dynamics and thermal conductivity of skutterudites CoSb<sub>3</sub> and IrSb<sub>3</sub> from first principles: Why IrSb<sub>3</sub> is a better thermal conductor than CoSb<sub>3</sub>. *Phys. Rev. B* **90**, 094302 (2014).
7. Guo, R., Wang, X. & Huang, B. Thermal conductivity of skutterudite CoSb<sub>3</sub> from first principles: Substitution and nanoengineering effects. *Sci. Rep.* **5**, 7806 (2015).
8. Jiang, P., Qian, X., Gu, X. & Yang, R. Probing Anisotropic Thermal Conductivity of Transition Metal Dichalcogenides MX<sub>2</sub> (M= Mo, W and X= S, Se) using Time-Domain Thermoreflectance. *Adv. Mater.* **29** (2017).